THE JOURNAL OF PHYSICAL CHEMISTRY LETTERS
A JOURNAL OF THE AMERICAN CHEMICAL SOCIETY

Open Access
This article is licensed under CC-BY-NC-ND 4.0

pubs.acs.org/JPCL
Letter

Exact Excited-State Functionals of the Asymmetric Hubbard Dimer

Sara Giarrusso* and Pierre-François Loos*

Cite This: J. Phys. Chem. Lett. 2023, 14, 8780−8786
Read Online

ACCESS | Metrics & More | Article Recommendations | Supporting Information

ABSTRACT: The exact functionals associated with the (singlet) ground state and the two singlet excited states of the asymmetric Hubbard dimer at half-filling are calculated using both Levy's constrained search and Lieb's convex formulation. While the ground-state functional is, as is commonly known, a convex function with respect to the density, the functional associated with the doubly excited state is found to be concave. Also, because the density-potential mapping associated with the first excited state is noninvertible, its "functional" is a partial, multivalued function composed of one concave and one convex branch that correspond to two separate domains of the external potential. Remarkably, it is found that, although the one-to-one mapping between density and external potential may not apply (as in the case of the first excited state), each state-specific energy and corresponding universal functional are "functions" whose derivatives are each other's inverse, just as in the ground state formalism.

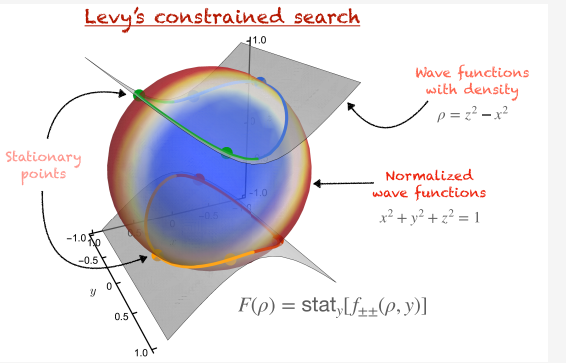

Downloaded via UNIV TOULOUSE III - PAUL SABATIER on October 9, 2023 at 07:35:38 (UTC).
See https://pubs.acs.org/sharingguidelines for options on how to legitimately share published articles.

Several decades after its foundation,[1] density-functional theory (DFT) still represents the main computational tool to perform quantum mechanical simulations of interest for pharmaceutical and technological applications.[2] Originally developed as a ground-state theory, it has been swiftly extended to calculate the lowest excited state of a given symmetry,[3−7] thereby obtaining excitation energies from differences of self-consistent field (ΔSCF) calculations. Notwithstanding the usefulness of such extension, for more general purposes, one usually relies on (linear-response) time-dependent (TD) DFT to describe excited states at the DFT level.[8−12] TDDFT is an in-principle exact theory, but in practice, it relies on approximations for the exchange-correlation kernel. A fundamental source of error underlying virtually all its implementations is adiabaticity (neglecting memory effects), while another type of error comes from the particular choice of the exchange-correlation functional, similar to ground-state Kohn−Sham DFT.[13] Within these approximations, TDDFT has seen important successes[14] but is also plagued by well-known shortcomings, e.g., for the description of double excitations or charge-transfer processes.[15−20]

Due to the relevance of these phenomena in photochemical applications or quantum-based technologies, alternative, time-independent theories have been developed. The most well-known is ensemble DFT (EDFT), based on an ensemble of equally weighted[21] or unequally weighted[22−24] densities, each coming from an individual quantum state rather than a pure-state density as in traditional DFT. In recent times, EDFT has undergone significant developments that are crucial to its advancement.[25−44] However, it suffers from the disadvantages that, to treat a high-lying excited state, it is usually required to include all lower-lying states in the ensemble and that the weight dependence of the exchange-correlation functional is hard to model. Another ensemble theory that has been receiving increasing attention and shares some of the problems of EDFT is *w*-ensemble one-body reduced density matrix functional theory.[45−49]

Concerning pure excited states, orbital-optimized DFT,[50−63] the extension to any excited state of the mentioned ΔSCF calculations, has been shown to be relatively successful for the calculation of classes of excitations where TDDFT typically fails,[55,56] although its theoretical underpinning is still in progress.

From a theoretical perspective, state-specific density-functional formalisms have been developed.[64−73] Some of these are complicated by the dependence of the functional on quantities other than the excited-state density and/or by the need for orthogonality constraints to inherit the variational character of the ground-state theory.[74]

In his seminal work, Görling[67] proposes a *stationarity* rather than a *minimum* principle to treat excited states. Building on Görling's work[69] and restricting the set of external potentials to Coulombic ones, Ayers et al. establish a one-to-one mapping between external potential and any of its associated stationary densities.[70−72] For a general external potential, this one-to-one

Received: July 24, 2023
Accepted: August 31, 2023
Published: September 22, 2023

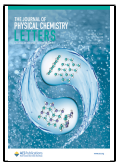

ACS Publications
© 2023 The Authors. Published by American Chemical Society

https://doi.org/10.1021/acs.jpclett.3c02052
J. Phys. Chem. Lett. 2023, 14, 8780−8786

mapping may not hold true.[50,75−77] However, none of these formalisms have revealed a fundamental dual relationship between excited-state energy and its corresponding state-specific functional similar to the one between the ground-state energy and the universal functional elucidated by Lieb.[78]

In turn, the present Letter provides an explicit case in which such a fundamental dual relationship carries through for excited states. Adopting Görling's stationarity principle[67] on Levy's constrained search[79] and Lieb's convex formulation,[78] we find for a simple model that, just as for the ground state, a given excited-state energy and its corresponding universal functional are functions whose derivatives are each other's inverse functions, a property described as "the essence of DFT".[80] Yet the "functional" associated with the first-excited state has some very peculiar mathematical properties.

Below, we first review the ground-state formalism. Consider the usual variational principle

$$E[v] = \min_{\Psi} \langle \Psi | \hat{H}_v | \Psi \rangle \tag{1}$$

where the minimization is performed over all normalized N-electron antisymetrized wave functions Ψ and the electronic Hamiltonian

$$\hat{H}_v = \hat{T} + \hat{V}_{ee} + \sum_{i=1}^{N} v(\boldsymbol{r}_i) \tag{2}$$

is composed of the kinetic energy operator $\hat{T}$, the electron repulsion operator $\hat{V}_{ee}$, and the external potential contribution.

The minimization in eq 1 can be split in two steps

$$\begin{aligned} E[v] &= \min_{\rho} \min_{\Psi \rightsquigarrow \rho} \langle \Psi | \hat{H}_v | \Psi \rangle \\ &= \min_{\rho} \left\{ F[\rho] + \int v(\boldsymbol{r}) \rho(\boldsymbol{r}) \mathrm{d}\boldsymbol{r} \right\} \end{aligned} \tag{3}$$

where in the second line we have introduced the Levy−Lieb or "universal" functional defined, via Levy's constrained search,[79] as

$$F[\rho] = \min_{\Psi \rightsquigarrow \rho} \langle \Psi | \hat{H}_0 | \Psi \rangle = \langle \Psi[\rho] | \hat{H}_0 | \Psi[\rho] \rangle \tag{4}$$

Note that the Hohenberg−Kohn,[1] Levy−Lieb,[78,79] or Lieb functional[78] differ in the density domain. We refer to any of them as the universal functional, although only the Lieb functional is properly convex in ρ.[80]

The Legendre−Fenchel transform of eq 3 delivers $F[\rho]$ from the maximization

$$F[\rho] = \max_{v} \left\{ E[v] - \int v(\boldsymbol{r}) \rho(\boldsymbol{r}) \mathrm{d}\boldsymbol{r} \right\} \tag{5}$$

exemplifying the duality between the functional $E[v]$, concave in the external potential v, and $F[\rho]$, convex in the density ρ.[78] Although technically discontinuous, $F[\rho]$ is "almost differentiable"[80] in that it may be approximated to any accuracy by a differentiable regularized functional.[81] Thus, assuming differentiability and carrying out the optimizations in eqs 3 and 5, one obtains

$$\frac{\delta F[\rho(\boldsymbol{r})]}{\delta \rho(\boldsymbol{r})} + v(\boldsymbol{r}) = 0 \tag{6a}$$

$$\frac{\delta E[v(\boldsymbol{r})]}{\delta v(\boldsymbol{r})} - \rho(\boldsymbol{r}) = 0 \tag{6b}$$

respectively.

We adopt the two-site Hubbard model at half-filling,[31,82−91] whose Hamiltonian reads

$$\hat{H} = -t \sum_{\sigma=\uparrow,\downarrow} (a_{0\sigma}^{\dagger} a_{1\sigma} + \text{h. c.}) + U \sum_{i=0}^{1} \hat{n}_{i\uparrow} \hat{n}_{i\downarrow} + \Delta v \frac{\hat{n}_1 - \hat{n}_0}{2} \tag{7}$$

where $t > 0$ is the hopping parameter, $U \geq 0$ is the on-site interaction parameter, $\hat{n}_{i\sigma} = a_{i\sigma}^{\dagger} a_{i\sigma}$ is the spin density operator on site i, $\hat{n}_i = \hat{n}_{i\uparrow} + \hat{n}_{i\downarrow}$ is the density operator on site i, and $\Delta v = v_1 - v_0$ (with $v_0 + v_1 = 0$) is the potential difference between the two sites.

Although simple, this model is able to describe the physics of partially filled narrow band gaps[82,83,85] and its two-site version has been used in the framework of site-occupation function theory to exemplify central concepts or test (new) density-functional methods by numerous authors.[31,84,86−91]

It is noteworthy to mention that for lattice systems, even in the case of the ground-state functional, the Hohenberg−Kohn theorem does not hold universally. While a potential does exist, it is not always unique. This aspect was recently highlighted by Penz and van Leeuwen.[92] However, in the context of linear Hubbard chains (like the one discussed in this paper where the chain is of length two), the uniqueness and thus the applicability of the Hohenberg−Kohn theorem are established by Theorem 17 in the aforementioned reference. This theorem provides a robust guarantee of uniqueness, ensuring that for linear Hubbard chains there is a unique potential associated with a given density. Notably, the present study and Schönhammer and Gunnarsson's original work also support this.[84]

At half filling ($N = 2$), we expand the Hamiltonian in the N-electron (spin-adapted) site basis $|0_\uparrow 0_\downarrow\rangle$, $(|0_\uparrow 1_\downarrow\rangle - |0_\downarrow 1_\uparrow\rangle)/\sqrt{2}$, and $|1_\uparrow 1_\downarrow\rangle$ to form the following Hamiltonian matrix

$$\mathbf{H} = \begin{pmatrix} U - \Delta v & -\sqrt{2}t & 0 \\ -\sqrt{2}t & 0 & -\sqrt{2}t \\ 0 & -\sqrt{2}t & U - \Delta v \end{pmatrix} \tag{8}$$

whose eigenvalues provide the singlet energies of the system. A generic singlet wave function can then be written as

$$|\Psi\rangle = x\,|0_\uparrow 0_\downarrow\rangle + y \frac{|0_\uparrow 1_\downarrow\rangle - |0_\downarrow 1_\uparrow\rangle}{\sqrt{2}} + z\,|1_\uparrow 1_\downarrow\rangle \tag{9}$$

with $-1 \leq x, y, z \leq 1$ and the normalization condition

$$x^2 + y^2 + z^2 = 1 \tag{10}$$

The energy is given by $E = T + V_{ee} + V$, with

$$T = -2\sqrt{2}\,t\,y(x + z) \tag{11a}$$

$$V_{ee} = U(x^2 + z^2) \tag{11b}$$

$$V = \rho \Delta v \tag{11c}$$

with

$$\rho = \left\langle \Psi \middle| \frac{\hat{n}_1 - \hat{n}_0}{2} \middle| \Psi \right\rangle = (z^2 - x^2) \tag{12}$$

https://doi.org/10.1021/acs.jpclett.3c02052
J. Phys. Chem. Lett. 2023, 14, 8780−8786

We call E_0, E_1, and E_2 the energies of the ground state, first (singly) excited state, and second (doubly) excited state, respectively. These are represented in Figure 1 as functions of

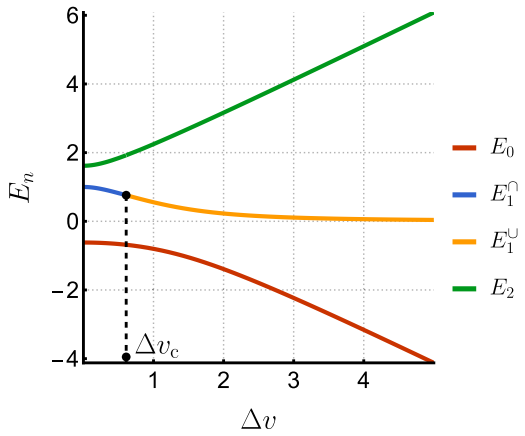

Figure 1. E_0, E_1, and E_2 as functions of Δv for $t = 1/2$ and $U = 1$. Note that E is an even function of Δv. E_1 is concave for $\Delta v < \Delta v_c$ and becomes convex for larger Δv values.

Δv for $t = 1/2$ and $U = 1$. It is worth noting that E_0 (red curve) and E_2 (green curve) are concave and convex with respect to Δv, respectively, for any value of t and U, while E_1 is concave for Δv smaller than the critical value Δv_c (blue curve labeled as $E_1^{\cap}$) and becomes convex for $\Delta v > \Delta v_c$ (yellow curve labeled as $E_1^{\cup}$).

The corresponding differences in (reduced) site occupation

$$\rho = \frac{\Delta n}{2} \tag{13}$$

for the ground state, ρ_0, first excited state, ρ_1, and second excited state, ρ_2, are represented in Figure 2. While the ground (red

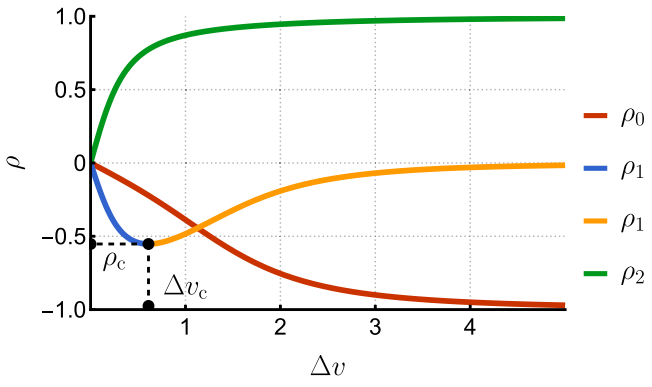

Figure 2. ρ as a function of Δv for $t = 1/2$ and $U = 1$ for the ground-state (ρ_0), the singly excited state (ρ_1), and the doubly excited states (ρ_2). ρ_1 reaches a critical value, ρ_c, at Δv_c. Note that ρ is an odd function of Δv.

curve) and the doubly excited (green curve) states have monotonic densities with respect to Δv for any t and U values, ρ_1 is nonmonotonic and reaches a critical value ρ_c at Δv_c before decaying to 0 as $\Delta v \to \infty$. In agreement with eq 6b, in the asymmetric Hubbard dimer, one finds

$$\frac{dE_0(\Delta v)}{d\Delta v} = 2\rho_0(\Delta v) \tag{14}$$

However, analogous relations hold true also for the two excited states, i.e.,

$$\frac{dE_1(\Delta v)}{d\Delta v} = 2\rho_1(\Delta v) \tag{15a}$$

$$\frac{dE_2(\Delta v)}{d\Delta v} = 2\rho_2(\Delta v) \tag{15b}$$

Substituting x and z in eqs 11a and 11b thanks to the normalization condition and the reduced site occupation difference defined in eqs 10 and 13, respectively, we obtain the four-branch function

$$f_{\pm\pm}(\rho, y) = -2ty(\pm\sqrt{1 - y^2 - \rho} \pm \sqrt{1 - y^2 + \rho}) + U(1 - y^2) \tag{16}$$

that one would minimize with respect to y to obtain the exact ground-state functional.[84,86,87] Although one technically deals with *functions* in the Hubbard dimer, we shall stick to the term *functional* to emphasize the formal analogy between site-occupation function theory and DFT, as customarily done in the literature.[49,87,90,93−95]

Rather than only minimizing eq 16 for a given ρ, we seek *all* stationary points[67] of $f_{\pm\pm}(\rho, y)$ with respect to y, i.e.,

$$F(\rho) = \underset{y}{\text{stat}}[f_{\pm\pm}(\rho, y)] \tag{17}$$

The choice of the variable over which to optimize in eq 17 is arbitrary and several choices are possible yielding various functions[86] other than $f_{\pm\pm}$, yet identical $F(\rho)$'s. A similar procedure can be carried out via an ensemble formalism,[22−24] as shown by Fromager and co-workers.[31−33]

Because, taken as whole, $f_{\pm\pm}$ is symmetric with respect to a change in sign of y, we restrict the discussion to the domain where $y \geq 0$, without a loss of generality. As shown in Figure 3, the branches f_{++} and f_{--} have one stationary point each for $y \geq 0$ (green square and red circle, respectively): the global minimum located at y_0 corresponds to the convex ground-state functional, $F_0(\rho) = f_{++}(\rho, y_0)$, while the global maximum at y_2 corresponds to the concave doubly excited-state functional, i.e., $F_2(\rho) = f_{--}(\rho, y_2)$ (see Figure 4). $F_0(\rho)$ and $F_2(\rho)$ merge at $\rho = 1$. The stationary points located at $-y_0$ and $-y_2$ are associated with opposite values of Δv.

For $\rho < \rho_c$, the branch f_{+-} has two stationary points (yellow diamonds): a local minimum at $y_1^{\cap}$ and a local maximum at $y_1^{\cup}$ that yield a concave branch $F_1^{\cap}(\rho) = f_{+-}(\rho, y_1^{\cap})$ (yellow curve in Figure 4) and a convex branch $F_1^{\cup}(\rho) = f_{+-}(\rho, y_1^{\cup})$ (blue curve in Figure 4) for the singly excited-state functional. As expected though, $F_1^{\cap}(\rho)$ and $F_1^{\cup}(\rho)$ lead to convex and concave energies, $E_1^{\cup}$ and $E_1^{\cap}$ (see Figure 1), respectively, preserving the property that the energy and the functional are conjugate functions.[80] Because the density-potential mapping associated with the first excited state is noninvertible (since, as seen in Figure 2, the same density ρ can be produced by two Δv values), its "functional" is a partial (i.e., defined for a subdomain of ρ), multivalued function constituted of one concave and one convex branch that correspond to two separate domains of the external potential. Again, the stationary points on f_{-+} located at $-y_1^{\cap}$ and $-y_1^{\cup}$ (blue triangles) are associated with opposite values of Δv. At $\rho = \rho_c$, $y_1^{\cap}$ and $y_1^{\cup}$ merge and disappear for larger ρ values. This critical value of the density decreases with respect to U to reach zero at $U = 0$, and $\rho_c \to 1$ as $U \to \infty$.

In accordance with eq 6a, the derivative of $F_0(\rho)$ with respect to ρ gives back Δv_0 as a function of ρ, i.e., the inverse of $\rho_0(\Delta v)$ plotted in Figure 2. Most notably, an analogous relation holds

https://doi.org/10.1021/acs.jpclett.3c02052
J. Phys. Chem. Lett. 2023, 14, 8780−8786

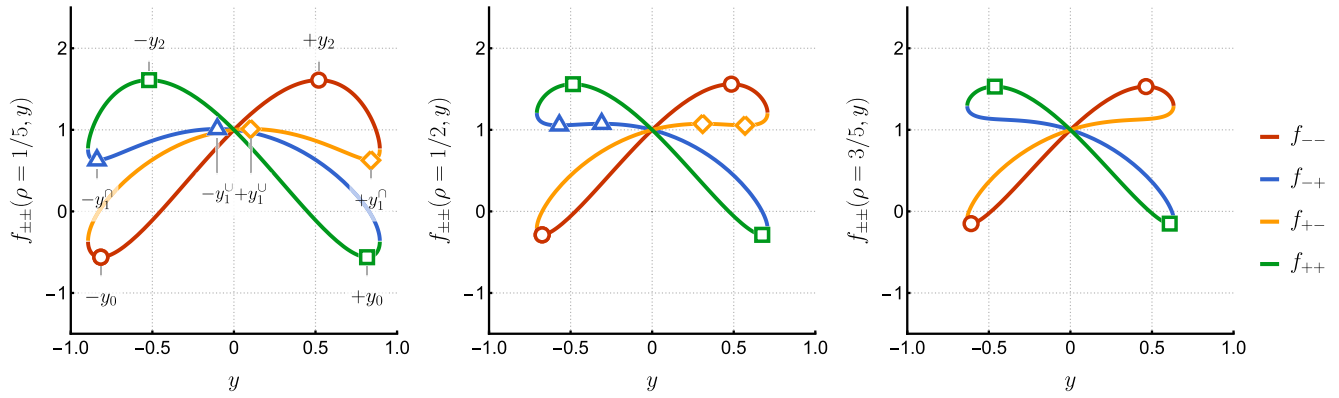

Figure 3. $f_{--}(\rho, y)$ (red), $f_{-+}(\rho, y)$ (blue), $f_{+-}(\rho, y)$ (yellow), and $f_{++}(\rho, y)$ (green) as functions of y for $t = 1/2$, $U = 1$, and $\rho = 1/5$ (left), $1/2$ (center), and $3/5$ (right). The markers indicate the positions of the stationary points on each branch. At $\rho = 3/5$ (right panel), the stationary points of f_{-+} and f_{+-} have disappeared as $\rho > \rho_c$ (see Figure 2).

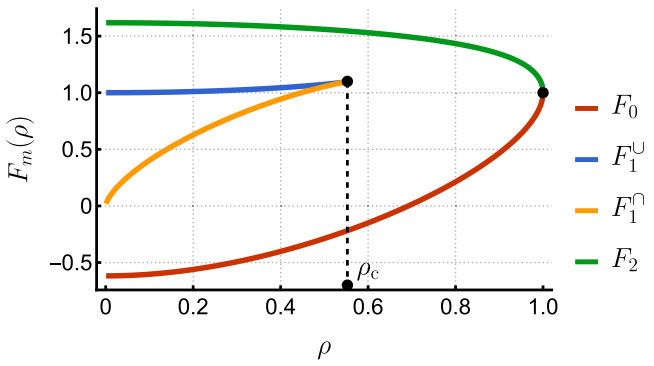

Figure 4. State-specific exact functionals $F_m(\rho)$ as functions of ρ for $t = 1/2$ and $U = 1$. The ground-state functional $F_0(\rho)$ (red) is convex with respect to ρ, and the singly excited-state multivalued functional $F_1(\rho)$ has one convex branch (blue) and one concave branch (yellow), each associated with a separate set of Δv values, while the doubly excited-state functional $F_2(\rho)$ (green) is concave. Note that F is an even function of ρ.

for the excited states. For the doubly excited state, we simply have

$$\frac{dF_2(\rho)}{d\rho} = -\Delta v_2(\rho) \tag{18}$$

In particular, for $\rho = 0$, we have $\Delta v_2 = 0$, while $\Delta v_2 \to \infty$ as $\rho \to 1$, similarly to Δv_0 (except that $\Delta v_0 \to -\infty$ as $\rho \to 1$).

For the first-excited state, which has a noninvertible density, $\rho_1(\Delta v)$ (see Figure 2), we still have

$$\frac{dF_1^{\cup}(\rho)}{d\rho} = -\Delta v_1^{\cup}(\rho) \tag{19a}$$

$$\frac{dF_1^{\cap}(\rho)}{d\rho} = -\Delta v_1^{\cap}(\rho) \tag{19b}$$

where $\Delta v_1^{\cup}(\rho)$ ranges from $-\Delta v_c$ (at $\rho = \rho_c$) to 0^- (for $\rho \to 0^+$), yielding the inverse of the blue curve in Figure 2, and $\Delta v_1^{\cap}(\rho)$ ranges from $-\infty$ (for $\rho \to 0^+$) to $-\Delta v_c$ (for $\rho = \rho_c$), yielding the inverse of the yellow curve in Figure 2.

The Levy constrained-search procedure is geometrically illustrated in Figure 5. The surface of the unit sphere corresponds to the normalized wave functions such that $x^2 + y^2 + z^2 = 1$, onto which we mapped the value of $T + V_{ee}$ as a function of x, y, and z. The gray parabolas correspond to the

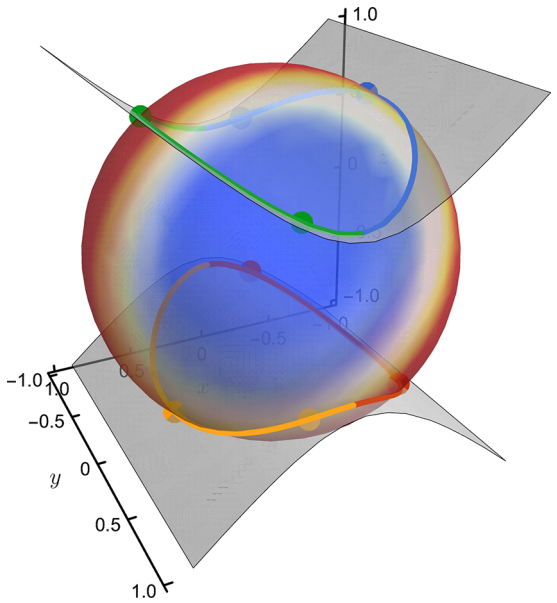

Figure 5. Illustration of the Levy constrained-search procedure for $t = 1/2$, $U = 1$, and $\rho = 1/5$. The value of $T + V_{ee}$ is mapped on the surface of the unit sphere, which represents the normalized wave functions. The gray parabolas correspond to density values $\rho = z^2 - x^2$. The four branches of $f_{\pm\pm}$ [eq 16] are represented as contours and correspond to the intersections of these three-dimensional objects. The dots locate the stationary points on each of these contours.

(potentially unnormalized) wave functions, yielding $\rho = z^2 - x^2$. Hence, the contours obtained by the intersection of these three-dimensional surfaces are the normalized wave functions, yielding $\rho = z^2 - x^2$. On these contours, one is looking for the points where $f_{\pm\pm}$ is stationary. These are represented by the colored dots in Figure 5 (see also Figure 3).

The exact functionals represented in Figure 4 can also be obtained by using the Lieb variational principle. To do so, let us define, for each singlet state, the function

$$f_m(\rho, \Delta v) = E_m - \Delta v \rho \tag{20}$$

However, instead of maximizing the previous expression for a given ρ as in eq 5, we seek its entire set of stationary points with respect to Δv for each m value, i.e.,

$$F_m(\rho) = \underset{\Delta v}{\text{stat}}[f_m(\rho, \Delta v)] \tag{21}$$

https://doi.org/10.1021/acs.jpclett.3c02052
J. Phys. Chem. Lett. 2023, 14, 8780−8786

Figure 6 shows f_m as a function of Δv at $\rho = 0$ and $\pm 1/2$ for each state and the location of the corresponding stationary points. For $\rho = 0$ (transparent curves), one recovers the energies E_m plotted in Figure 1. The values of the functions f_m at their stationary points (red circle, blue triangle, and green square at $\Delta v = 0$) correspond to the initial values of F_0, $F_1^{\cup}$, and F_2 in Figure 4. For $\rho = 1/2$, f_0 (solid red curve) and f_2 (solid green curve) have a single extremum: a maximum and a minimum, yielding the ground- and second-excited-state functionals, $F_0(\rho)$ and $F_2(\rho)$, respectively, as depicted in Figure 4. The blue curve f_1 exhibits a local maximum and minimum that correspond to the two branches of the multivalued functional associated with the first-excited state, $F_1^{\cap}(\rho)$ and $F_1^{\cup}(\rho)$, respectively.

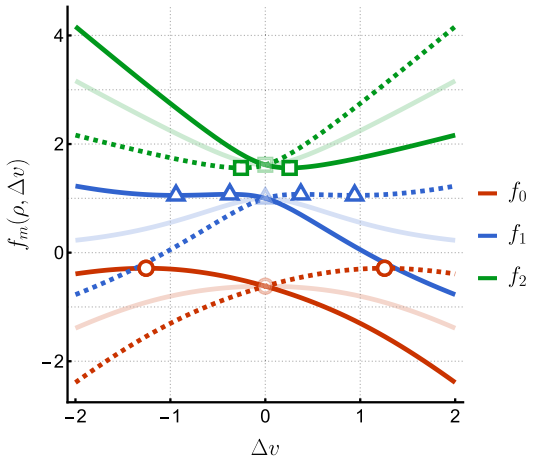

Figure 6. $f_m(\rho, \Delta v)$ as a function of Δv for $t = 1/2$, $U = 1$, and $\rho = \pm 1/2$: ground state ($m = 0$), singly excited state ($m = 1$), and doubly excited state ($m = 2$). The markers indicate the positions of the stationary points. The transparent curves correspond to $\rho = 0$. In this case, the linear term $-\Delta v\rho$ in eq 5 vanishes, and the energy E_m is recovered (see Figure 1). For $\rho = 1/2$ (solid curves), the linear term shifts the maxima of E_0 and E_1 (red circle and blue triangle, respectively) toward $\Delta v < 0$ and the minimum of E_2 (green square) toward $\Delta v > 0$. Moreover, a local minimum in f_1 (the outermost blue triangle) appears. The situation is exactly mirrored for $\rho = -1/2$ (dashed curves).

In practice, Lieb's formulation has a very neat geometric illustration in the Hubbard dimer. The total energies E_m are "tipped" by the addition of the linear term $-\Delta v\rho$, which shifts their extrema: the maxima of E_0 and E_1 toward $\Delta v < 0$ and the minimum of E_2 toward $\Delta v > 0$. Moreover, in the case of the first-excited state, the linear curve $-\Delta v\rho$ shifts the energy in such a way that as soon as $\rho > 0$, a local minimum appears (outermost blue triangle) in f_1. This minimum and the maximum gradually get closer as ρ increases until they merge at $\rho = \rho_c$, f_1 becoming monotonic with no stationary points for $\rho > \rho_c$. The situation is exactly mirrored for $\rho = -1/2$ (dashed curves).

The present Letter reports the exact functionals for the ground and (singlet) excited states of the asymmetric Hubbard dimer at half-filling. To the best of our knowledge, this is the first time that exact function(al)s corresponding to singlet (non-degenerate) excited states are computed. While the ground-state functional is well-known to be a convex function with respect to the site-occupation difference, the functional associated with the highest-double-excited state is found to be concave. Additionally, and more importantly, we find that the "functional" for the first-excited state is a partial, multivalued function of the density that is constructed from one concave and one convex branch associated with two separate domains of the external potential. Finally, Levy's constrained search and Lieb's convex formulation are found to be entirely consistent with one another, yielding the same exact functionals [eqs 17 and 21] and, even more remarkably, the duality properties of the ground state appear to be shared by the excited states of this model. These findings may provide insight into the challenges of constructing state-specific excited-state density functionals for general applications in electronic structure theory.

■ ASSOCIATED CONTENT

Supporting Information

The Supporting Information is available free of charge at https://pubs.acs.org/doi/10.1021/acs.jpclett.3c02052.

Transparent Peer Review report available (PDF)

■ AUTHOR INFORMATION

Corresponding Authors

Sara Giarrusso − *Laboratoire de Chimie et Physique Quantiques (UMR 5626), Université de Toulouse, CNRS, UPS, 31062 Toulouse, France*; Email: sgiarrusso@irsamc.ups-tlse.fr

Pierre-François Loos − *Laboratoire de Chimie et Physique Quantiques (UMR 5626), Université de Toulouse, CNRS, UPS, 31062 Toulouse, France*; orcid.org/0000-0003-0598-7425; Email: loos@irsamc.ups-tlse.fr

Complete contact information is available at: https://pubs.acs.org/10.1021/acs.jpclett.3c02052

Notes

The authors declare no competing financial interest.

■ ACKNOWLEDGMENTS

This project has received funding from the European Research Council (ERC) under the European Union's Horizon 2020 research and innovation program (Grant agreement No. 863481).

■ REFERENCES

(1) Hohenberg, P.; Kohn, W. Inhomogeneous electron gas. *Phys. Rev.* **1964**, *136*, B864−B871.

(2) Teale, A. M.; et al. DFT exchange: sharing perspectives on the workhorse of quantum chemistry and materials science. *Phys. Chem. Chem. Phys.* **2022**, *24*, 28700−28781.

(3) Gunnarsson, O.; Lundqvist, B. I. Exchange and correlation in atoms, molecules, and solids by the spin-density-functional formalism. *Phys. Rev. B* **1976**, *13*, 4274−4298.

(4) Ziegler, T.; Rauk, A.; Baerends, E. J. On the calculation of multiplet energies by the Hartree-Fock-Slater method. *Theor. Chem. Acc.* **1977**, *43*, 261−271.

(5) Gunnarsson, O.; Jonson, M.; Lundqvist, B. Descriptions of exchange and correlation effects in inhomogeneous electron systems. *Phys. Rev. B* **1979**, *20*, 3136.

(6) von Barth, U. Local-density theory of multiplet structure. *Phys. Rev. A* **1979**, *20*, 1693.

(7) Englisch, H.; Fieseler, H.; Haufe, A. Density-functional calculations for excited-state energies. *Phys. Rev. A* **1988**, *37*, 4570.

(8) Runge, E.; Gross, E. K. U. Density-Functional Theory for Time-Dependent Systems. *Phys. Rev. Lett.* **1984**, *52*, 997−1000.

(9) Appel, H.; Gross, E. K.; Burke, K. Excitations in time-dependent density-functional theory. *Phys. Rev. Lett.* **2003**, *90*, 043005.

(10) Burke, K.; Werschnik, J.; Gross, E. K. U. Time-dependent density functional theory: Past, present, and future. *J. Chem. Phys.* **2005**, *123*, 062206.

(11) Casida, M.; Huix-Rotllant, M. Progress in Time-Dependent Density-Functional Theory. *Annu. Rev. Phys. Chem.* **2012**, *63*, 287.
(12) Huix-Rotllant, M.; Ferré, N.; Barbatti, M. *Quantum Chemistry and Dynamics of Excited States*; John Wiley & Sons, Ltd.: 2020; Chapter 2, pp 13−46.
(13) Kohn, W.; Sham, L. J. Self-Consistent Equations Including Exchange and Correlation Effects. *Phys. Rev.* **1965**, *140*, A1133−A1138.
(14) Jacquemin, D.; Wathelet, V.; Perpete, E. A.; Adamo, C. Extensive TD-DFT benchmark: singlet-excited states of organic molecules. *J. Chem. Theory Comput.* **2009**, *5*, 2420−2435.
(15) Tozer, D. J.; Amos, R. D.; Handy, N. C.; Roos, B. O.; Serrano-Andres, L. Does Density Functional Theory Contribute to the Understanding of Excited States of Unsaturated Organic Compounds? *Mol. Phys.* **1999**, *97*, 859−868.
(16) Tozer, D. J.; Handy, N. C. On the Determination of Excitation Energies Using Density Functional Theory. *Phys. Chem. Chem. Phys.* **2000**, *2*, 2117−2121.
(17) Dreuw, A.; Weisman, J. L.; Head-Gordon, M. Long-Range Charge-Transfer Excited States in Time-Dependent Density Functional Theory Require Non-Local Exchange. *J. Chem. Phys.* **2003**, *119*, 2943−2946.
(18) Maitra, N. T.; Zhang, F.; Cave, R. J.; Burke, K. Double excitations within time-dependent density functional theory linear response. *J. Chem. Phys.* **2004**, *120*, 5932.
(19) Levine, B. G.; Ko, C.; Quenneville, J.; Martinez, T. J. Conical Intersections and Double Excitations in Time-Dependent Density Functional Theory. *Mol. Phys.* **2006**, *104*, 1039−1051.
(20) Maitra, N. T. Charge Transfer In Time-Dependent Density Functional Theory. *J. Phys. Cond. Matt.* **2017**, *29*, 423001.
(21) Theophilou, A. K. The Energy Density Functional Formalism for Excited States. *J. Phys. C* **1979**, *12*, 5419−5430.
(22) Gross, E. K. U.; Oliveira, L. N.; Kohn, W. Rayleigh-Ritz Variational Principle for Ensembles of Fractionally Occupied States. *Phys. Rev. A* **1988**, *37*, 2805−2808.
(23) Gross, E. K. U.; Oliveira, L. N.; Kohn, W. Density-Functional Theory for Ensembles of Fractionally Occupied States. I. Basic Formalism. *Phys. Rev. A* **1988**, *37*, 2809−2820.
(24) Oliveira, L. N.; Gross, E. K. U.; Kohn, W. Density-Functional Theory for Ensembles of Fractionally Occupied States. II. Application to the He Atom. *Phys. Rev. A* **1988**, *37*, 2821−2833.
(25) Pribram-Jones, A.; Yang, Z.-h.; Trail, J. R.; Burke, K.; Needs, R. J.; Ullrich, C. A. Excitations and Benchmark Ensemble Density Functional Theory for Two Electrons. *J. Chem. Phys.* **2014**, *140*, 18A541.
(26) Yang, Z.-H.; Trail, J. R.; Pribram-Jones, A.; Burke, K.; Needs, R. J.; Ullrich, C. A. Exact and Approximate Kohn-Sham Potentials in Ensemble Density-Functional Theory. *Phys. Rev. A* **2014**, *90*, 042501.
(27) Yang, Z.-H.; Pribram-Jones, A.; Burke, K.; Ullrich, C. A. Direct Extraction of Excitation Energies from Ensemble Density-Functional Theory. *Phys. Rev. Lett.* **2017**, *119*, 033003.
(28) Sagredo, F.; Burke, K. Accurate Double Excitations from Ensemble Density Functional Calculations. *J. Chem. Phys.* **2018**, *149*, 134103.
(29) Filatov, M. In *Density-Functional Methods for Excited States*; Ferré, N., Filatov, M., Huix-Rotllant, M., Eds.; Springer International Publishing: Cham, 2016; pp 97−124.
(30) Senjean, B.; Knecht, S.; Jensen, H. J. A.; Fromager, E. Linear Interpolation Method in Ensemble Kohn-Sham and Range-Separated Density-Functional Approximations for Excited States. *Phys. Rev. A* **2015**, *92*, 012518.
(31) Deur, K.; Mazouin, L.; Fromager, E. Exact Ensemble Density Functional Theory for Excited States in a Model System: Investigating the Weight Dependence of the Correlation Energy. *Phys. Rev. B* **2017**, *95*, 035120.
(32) Deur, K.; Mazouin, L.; Senjean, B.; Fromager, E. Exploring Weight-Dependent Density-Functional Approximations for Ensembles in the Hubbard Dimer. *Eur. Phys. J. B* **2018**, *91*, 162.
(33) Deur, K.; Fromager, E. Ground and excited energy levels can be extracted exactly from a single ensemble density-functional theory calculation. *J. Chem. Phys.* **2019**, *150*, 094106.
(34) Marut, C.; Senjean, B.; Fromager, E.; Loos, P.-F. Weight dependence of local exchange−correlation functionals in ensemble density-functional theory: double excitations in two-electron systems. *Faraday Discuss.* **2020**, *224*, 402−423.
(35) Loos, P.-F.; Fromager, E. A weight-dependent local correlation density-functional approximation for ensembles. *J. Chem. Phys.* **2020**, *152*, 214101.
(36) Fromager, E. Individual Correlations in Ensemble Density Functional Theory: State- and Density-Driven Decompositions without Additional Kohn-Sham Systems. *Phys. Rev. Lett.* **2020**, *124*, 243001.
(37) Cernatic, F.; Senjean, B.; Robert, V.; Fromager, E. Ensemble Density Functional Theory of Neutral and Charged Excitations. *Top. Curr. Chem.* **2022**, *380*, 4.
(38) Gould, T.; Pittalis, S. Hartree and Exchange in Ensemble Density Functional Theory: Avoiding the Nonuniqueness Disaster. *Phys. Rev. Lett.* **2017**, *119*, 243001.
(39) Gould, T.; Kronik, L.; Pittalis, S. Charge Transfer Excitations from Exact and Approximate Ensemble Kohn-Sham Theory. *J. Chem. Phys.* **2018**, *148*, 174101.
(40) Gould, T.; Pittalis, S. Density-Driven Correlations in Many-Electron Ensembles: Theory and Application for Excited States. *Phys. Rev. Lett.* **2019**, *123*, 016401.
(41) Gould, T.; Stefanucci, G.; Pittalis, S. Ensemble Density Functional Theory: Insight from the Fluctuation-Dissipation Theorem. *Phys. Rev. Lett.* **2020**, *125*, 233001.
(42) Gould, T.; Kronik, L.; Pittalis, S. Double excitations in molecules from ensemble density functionals: Theory and approximations. *Phys. Rev. A* **2021**, *104*, 022803.
(43) Gould, T.; Hashimi, Z.; Kronik, L.; Dale, S. G. Single Excitation Energies Obtained from the Ensemble "HOMO−LUMO Gap": Exact Results and Approximations. *J. Phys. Chem. Lett.* **2022**, *13*, 2452−2458.
(44) Gould, T.; Kooi, D. P.; Gori-Giorgi, P.; Pittalis, S. Electronic Excited States in Extreme Limits via Ensemble Density Functionals. *Phys. Rev. Lett.* **2023**, *130*, 106401.
(45) Schilling, C.; Pittalis, S. Ensemble reduced density matrix functional theory for excited states and hierarchical generalization of Pauli's exclusion principle. *Phys. Rev. Lett.* **2021**, *127*, 023001.
(46) Liebert, J.; Castillo, F.; Labbé, J.-P.; Schilling, C. Foundation of one-particle reduced density matrix functional theory for excited states. *J. Chem. Theory Comput.* **2022**, *18*, 124−140.
(47) Liebert, J.; Schilling, C. An exact one-particle theory of bosonic excitations: From a generalized Hohenberg-Kohn theorem to convexified N-representability. *New J. Phys.* **2023**, *25*, 013009.
(48) Liebert, J.; Schilling, C. Deriving density-matrix functionals for excited states. *SciPost Phys.* **2023**, *14*, 120.
(49) Liebert, J.; Chaou, A. Y.; Schilling, C. Refining and relating fundamentals of functional theory. *J. Chem. Phys.* **2023**, *158*, 214108.
(50) Perdew, J. P.; Levy, M. Extrema of the Density Functional for the Energy: Excited States from the Ground-State Theory. *Phys. Rev. B* **1985**, *31*, 6264−6272.
(51) Kowalczyk, T.; Tsuchimochi, T.; Chen, P.-T.; Top, L.; Van Voorhis, T. Excitation energies and Stokes shifts from a restricted open-shell Kohn-Sham approach. *J. Chem. Phys.* **2013**, *138*, 164101.
(52) Gilbert, A. T.; Besley, N. A.; Gill, P. M. Self-consistent field calculations of excited states using the maximum overlap method (MOM). *J. Phys. Chem. A* **2008**, *112*, 13164−13171.
(53) Barca, G. M. J.; Gilbert, A. T. B.; Gill, P. M. W. Simple Models for Difficult Electronic Excitations. *J. Chem. Theory. Comput.* **2018**, *14*, 1501−1509.
(54) Barca, G. M. J.; Gilbert, A. T. B.; Gill, P. M. W. Excitation Number: Characterizing Multiply Excited States. *J. Chem. Theory. Comput.* **2018**, *14*, 9−13.
(55) Hait, D.; Head-Gordon, M. Excited State Orbital Optimization via Minimizing the Square of the Gradient: General Approach and Application to Singly and Doubly Excited States via Density Functional Theory. *J. Chem. Theory Comput.* **2020**, *16*, 1699−1710.

https://doi.org/10.1021/acs.jpclett.3c02052
J. Phys. Chem. Lett. 2023, 14, 8780−8786

(56) Hait, D.; Head-Gordon, M. Orbital Optimized Density Functional Theory for Electronic Excited States. *J. Phys. Chem. Lett.* **2021**, *12*, 4517−4529.
(57) Shea, J. A. R.; Neuscamman, E. Communication: A Mean Field Platform for Excited State Quantum Chemistry. *J. Chem. Phys.* **2018**, *149*, 081101.
(58) Shea, J. A. R.; Gwin, E.; Neuscamman, E. A Generalized Variational Principle with Applications to Excited State Mean Field Theory. *J. Chem. Theory Comput.* **2020**, *16*, 1526−1540.
(59) Hardikar, T. S.; Neuscamman, E. A self-consistent field formulation of excited state mean field theory. *J. Chem. Phys.* **2020**, *153*, 164108.
(60) Levi, G.; Ivanov, A. V.; Jónsson, H. Variational Density Functional Calculations of Excited States via Direct Optimization. *J. Chem. Theory Comput.* **2020**, *16*, 6968−6982.
(61) Carter-Fenk, K.; Herbert, J. M. State-Targeted Energy Projection: A Simple and Robust Approach to Orbital Relaxation of Non-Aufbau Self-Consistent Field Solutions. *J. Chem. Theory Comput.* **2020**, *16*, 5067−5082.
(62) Toffoli, D.; Quarin, M.; Fronzoni, G.; Stener, M. Accurate Vertical Excitation Energies of BODIPY/Aza-BODIPY Derivatives from Excited-State Mean-Field Calculations. *J. Phys. Chem. A* **2022**, *126*, 7137−7146.
(63) Schmerwitz, Y. L. A.; Levi, G.; Jónsson, H. Calculations of Excited Electronic States by Converging on Saddle Points Using Generalized Mode Following. *J. Chem. Theory Comput.* **2023**, *19*, 3634−3651.
(64) Görling, A. Density-functional theory for excited states. *Phys. Rev. A* **1996**, *54*, 3912.
(65) Nagy, A. Optimized Potential Method for Ensembles of Excited States. *Int. J. Quantum Chem.* **1998**, *69*, 247−254.
(66) Levy, M.; Nagy, A. Variational Density-Functional Theory for an Individual Excited State. *Phys. Rev. Lett.* **1999**, *83*, 4361−4364.
(67) Görling, A. Density-functional theory beyond the Hohenberg-Kohn theorem. *Phys. Rev. A* **1999**, *59*, 3359−3374.
(68) Zhang, F.; Burke, K. Adiabatic connection for near degenerate excited states. *Phys. Rev. A* **2004**, *69*, 052510.
(69) Ayers, P. W.; Levy, M. Time-independent (static) density-functional theories for pure excited states: Extensions and unification. *Phys. Rev. A* **2009**, *80*, 012508.
(70) Ayers, P. W.; Levy, M.; Nagy, A. Time-independent density-functional theory for excited states of Coulomb systems. *Phys. Rev. A* **2012**, *85*, 042518.
(71) Ayers, P. W.; Levy, M.; Nagy, Á. Communication: Kohn-Sham theory for excited states of Coulomb systems. *J. Chem. Phys.* **2015**, *143*, 191101.
(72) Ayers, P. W.; Levy, M.; Nagy, A. Time-independent density functional theory for degenerate excited states of Coulomb systems. *Theor. Chem. Acc.* **2018**, *137*, 152.
(73) Garrigue, L. Building Kohn−Sham Potentials for Ground and Excited States. *Arch. Rational Mech. Anal.* **2022**, *245*, 949−1003.
(74) Lieb, E. H. In *Density Functional Methods in Physics*; Dreizler, R. M., da Providencia, J., Eds.; Plenum: New York, 1985; pp 31−80.
(75) Gaudoin, R.; Burke, K. Lack of Hohenberg-Kohn Theorem for Excited States. *Phys. Rev. Lett.* **2004**, *93*, 173001.
(76) Samal, P.; Harbola, M. K. Local-density approximation for the exchange energy functional in excited-state density functional theory. *J. Phys. B At. Mol. Opt. Phys.* **2005**, *38*, 3765.
(77) Samal, P.; Harbola, M. K.; Holas, A. Density-to-potential map in time-independent excited-state density-functional theory. *Chem. Phys. Lett.* **2006**, *419*, 217−222.
(78) Lieb, E. H. Density Functionals For Coulomb Systems. *Int. J. Quantum Chem.* **1983**, *24*, 243.
(79) Levy, M. Universal Variational Functionals Of Electron Densities, First-Order Density Matrices, And Natural Spin-Orbitals And Solution Of The V-Representability Problem. *Proc. Natl. Acad. Sci. U.S.A.* **1979**, *76*, 6062.
(80) Helgaker, T.; Teale, A. M. *The Physics and Mathematics of Elliott Lieb*; EMS Press: 2022; pp 527−559.
(81) Kvaal, S.; Ekström, U.; Teale, A. M.; Helgaker, T. Differentiable but exact formulation of density-functional theory. *J. Chem. Phys.* **2014**, *140*, 18A518.
(82) Hubbard, J. Electron correlations in narrow energy bands. *Proc. Math. Phys. Eng.* **1963**, *276*, 238−257.
(83) Lieb, E. H.; Wu, F. Absence of Mott Transition in an Exact Solution of the Short-Range, One-Band Model in One Dimension. *Phys. Rev. Lett.* **1968**, *20*, 1445.
(84) Schonhammer, K.; Gunnarsson, O. Discontinuity of the exchange-correlation potential in density functional theory. *J. Phys. C* **1987**, *20*, 3675−3689.
(85) Montorsi, A. *The Hubbard Model: A Reprint Volume*; World Scientific, 1992.
(86) Carrascal, D. J.; Ferrer, J.; Smith, J. C.; Burke, K. The Hubbard Dimer: A Density Functional Case Study of a Many-Body Problem. *J. Phys.: Condens. Matter* **2015**, *27*, 393001.
(87) Cohen, A. J.; Mori-Sánchez, P. Landscape of an Exact Energy Functional. *Phys. Rev. A* **2016**, *93*, 042511.
(88) Ying, Z.-J.; Brosco, V.; Lopez, G. M.; Varsano, D.; Gori-Giorgi, P.; Lorenzana, J. Anomalous scaling and breakdown of conventional density functional theory methods for the description of Mott phenomena and stretched bonds. *Phys. Rev. B* **2016**, *94*, 075154.
(89) Smith, J. C.; Pribram-Jones, A.; Burke, K. Exact Thermal Density Functional Theory for a Model System: Correlation Components and Accuracy of the Zero-Temperature Exchange-Correlation Approximation. *Phys. Rev. B* **2016**, *93*, 245131.
(90) Senjean, B.; Tsuchiizu, M.; Robert, V.; Fromager, E. Local density approximation in site-occupation embedding theory. *Mol. Phys.* **2017**, *115*, 48−62.
(91) Carrascal, D. J.; Ferrer, J.; Maitra, N.; Burke, K. Linear Response Time-Dependent Density Functional Theory of the Hubbard Dimer. *Eur. Phys. J. B* **2018**, *91*, 142.
(92) Penz, M.; van Leeuwen, R. Density-functional theory on graphs. *J. Chem. Phys.* **2021**, *155*, 244111.
(93) Capelle, K.; Campo, V. L., Jr Density functionals and model Hamiltonians: Pillars of many-particle physics. *Phys. Rep.* **2013**, *528*, 91−159.
(94) Dimitrov, T.; Appel, H.; Fuks, J. I.; Rubio, A. Exact maps in density functional theory for lattice models. *New J. Phys.* **2016**, *18*, 083004.
(95) Giarrusso, S.; Pribram-Jones, A. Comparing correlation components and approximations in Hartree−Fock and Kohn−Sham theories via an analytical test case study. *J. Chem. Phys.* **2022**, *157*, 054102.

https://doi.org/10.1021/acs.jpclett.3c02052
J. Phys. Chem. Lett. 2023, 14, 8780−8786